Direct-to-indirect transition observed in quantum dot photoluminescence with nanoprobe indentation

Kazunari Ozasa,[a] Mizuo Maeda, and Masahiko Hara
RIKEN, 2-1 Hirosawa, Wako, Saitama 351-0198, Japan

Hiroki Kakoi, Lixia Xu, Yuan-Hua Liang, and Yoshio Arai
Saitama University, 255 Shimo-ookubo, Sakuraku, Saitama 338-8570, Japan

(Received 11 August 2008; accepted 7 October 2008; published 1 April 2009)

Photoluminescence (PL) of InGaAs/GaAs quantum dots (QDs) is found to be enhanced and then quenched by localized-strain effects induced by the indentation of a nanoprobe. By using a nanoprobe with a flat cylindrical apex of 600 nm in radius, the quench of individual fine PL peaks originating from single QDs was analyzed to obtain the relation between the QD location relative to the nanoprobe and the indentation force required to quench the PL. By analyzing direct-to-indirect transition in the band lineup of the QDs and surrounding GaAs matrix through numerical simulation, the authors concluded that the PL quench should be attributed to the crossover of the Γ band of InGaAs and the *X* band of InGaAs. The bowing parameter of the InGaAs *X* band of 1050 ± 50 meV was deduced by fitting the simulation result to the experimental data. © *2009 American Vacuum Society.* [DOI: 10.1116/1.3010731]

I. INTRODUCTION

Localized strain is a matter of importance from the viewpoint to improve physical parameters such as mobility or energy band gap beyond that of native unstrained materials.[1,2] The most typical example of nanostructures with localized strains is strain-induced/self-assembled quantum dots (QDs),[3,4] whose energy band gap is affected severely by lattice-mismatch strain. By applying a localized strain externally onto such nanostructures, e.g., through the indentation of a nanoprobe, a further change is evoked in their physical properties, especially in their optical properties. In our previous study,[5–7] we have already reported a remarkable photoluminescence (PL) enhancement by nanoprobe-induced localized-strain effects on InGaAs/GaAs QDs and made it clear that the enhancement is due to the accumulation of photoexcited holes at a certain area close to the nanoprobe edge (in the case that the nanoprobe has a flat apex).

When the nanoprobe-indentation force is further increased, the PL peaks once enhanced by the indentation start decreasing and finally disappear (quenched). This behavior cannot be explained by the reversal process of enhancement, i.e., the hole accumulation is not canceled out by further indentation. Direct-to-indirect transition in the band lineup of the QDs and surrounding GaAs matrix is the most probable mechanism that quenches the PL since the QDs become nonradiative by the transition.

In this article, we focus on the quench of fine PL peaks at higher nanoprobe-indentation forces, which has not been explained in our previous study. The Γ- and *X*-band behaviors of the InGaAs QDs and GaAs matrix were analyzed by numerical strain/energy-level calculations. The direct-to-indirect transition condition derived by the numerical calculations was elucidated by the comparison with the experimental data. From the fitting of calculations and experimental data, the bowing parameter of the InGaAs *X* band was deduced.

II. EXPERIMENTS

The QDs measured in this study were strain-induced self-assembled $In_{0.5}Ga_{0.5}As/GaAs$ QDs prepared with chemical beam epitaxy (480 °C).[8] The QDs have a pyramidlike shape[9] with approximately 20 nm in base width and 7 nm in height. The density of QDs was $(5-6) \times 10^{10}$ cm^{-2}. They were embedded in a GaAs capping layer of 50 nm in thickness. Since the QDs distribute randomly in a plane at 50 nm depth, the exact location of QDs cannot be observed directly by a microscope.

An optical fiber nanoprobe with a flat and cylindrical apex (600 nm in radius) was indented onto the sample surface by means of a voltage-controlled piezoelectric nanoprobe scanner [lead zirconate titanate; $PbZr_xTi_{1-x}O_3$ (PZT) scanner] in our scanning-tunneling-microscope–PL combination system.[10] The measurements were performed at low temperature (liquid helium cooled, approximately 10 K) under ultrahigh vacuum (approximately 4×10^{-9} Pa). A 45°-incident laser beam (frequency doubled yttrium aluminum garnet laser, 532 nm, 540 mW/cm^2) excited the QDs/GaAs optically, and PL from the QDs was collected through an aperture at the nanoprobe apex. Figure 1(a) shows typical full PL spectra of the QDs observed with nanoprobe indentation. The indentation force was increased stepwise by PZT voltage control. The relation between the PZT voltage and indentation force was evaluated separately by using a high-sensitivity load cell (Tokyo Sokki, CLS-1NLS). One step of the indentation was chosen as 57 μN increase. At each step of indentation, the PL spectrum was measured with a monochromator (SPEX, 270M) and liquid-nitrogen-cooled charge coupled device (SPEX, CCD-2000), with 5.0 s integration.

[a]Electronic mail: ozasa@riken.jp

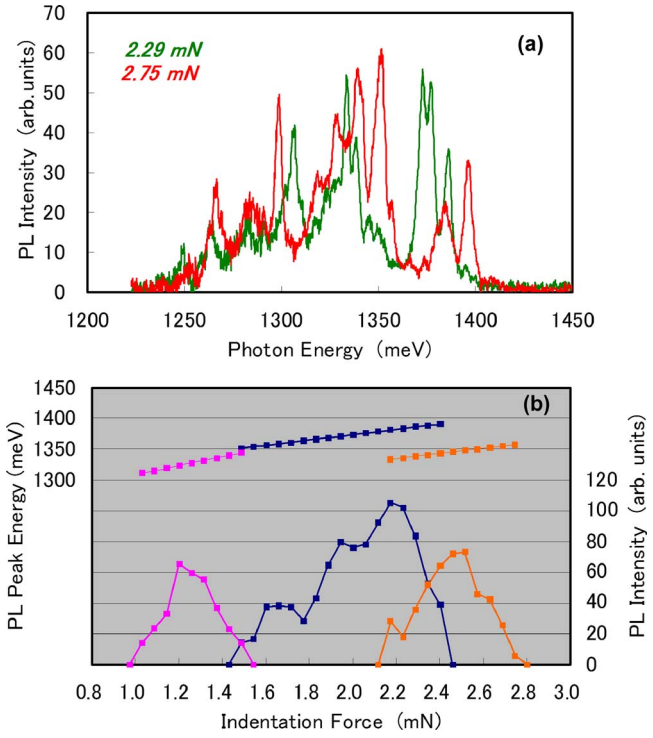

FIG. 1. (Color online) (a) Two examples of full PL spectrum of the QDs with indentation forces of 2.28 and 2.75 mN. (b) Three examples of fine PL peaks under nanoprobe indentation, i.e., dependence of peak energy and intensity on the indentation force.

III. SIMULATIONS

In numerical calculation, strain distribution was analyzed on the basis of elastic small deformation theory with finite element method. Since the size of the nanoprobe apex was more than one order of magnitude larger than the size of the QDs, we separated the calculation into four steps: (1) indentation-induced strain distribution in uniform GaAs matrix (without the QDs) was calculated for $4.0(x)\times 2.0(y)\times 2.0(z)\ \mu\text{m}^3$, (2) the indentation-induced strain inside/around a single QD (pyramidal shape of 7 nm in height and 20 nm in base width) at a certain horizontal distance away from the nanoprobe center (hereafter, the location of QD is represented as 600 nm in QD location, which means that the QD is located at the distance of 600 nm away horizontally from the nanoprobe center at 50 nm in depth) was calculated for $200\times 100\times 140\ \text{nm}^3$ with applying the displacement boundary condition derived from the first step, (3) the lattice-mismatched strain inside/around a single QD was calculated (separately from indentation-induced strains) for $50\times 25\times 150\ \text{nm}^3$ with a periodic boundary condition along the x and y directions, and (4) the strains derived from (2) and (3) were superimposed to finalize the strain distribution induced by lattice mismatch and nanoprobe indentation. The details of strain calculation can be found in our previous reports.[6]

Band gap shift induced by the strain distribution was calculated with the 6×6 strain Hamiltonian of Pikus and Bir[11] for valence band behavior. Γ-band shifts and X-band shifts were calculated with the following equations, respectively:

TABLE I. Material parameters used in the simulation. All the parameters were taken from Ref. 14 except for Ξ_u, Ξ_d, and valence band offset (VBO), taken from Refs. 12 and 13.

	GaAs	InGaAs
a (Å)	5.653 25	5.863 88
c_{11} (GPa)	122.10	101.92
c_{12} (GPa)	56.60	50.70
c_{44} (GPa)	60.00	49.39
a_c (eV)	−7.17	−6.74
a_v (eV)	−1.16	−1.08
b (eV)	−2.00	−1.90
d (eV)	−4.80	−4.18
Δ_0 (eV)	0.341	0.329
Ξ_d (eV)	−0.87	−0.37
Ξ_u (eV)	8.61	6.47
$E_g(T)$ (eV)	1.518 75	0.826 64
$E_g(X)$ (eV)	1.980 79	1.346 37
VBO (eV)	−6.806	−6.680

$$\Delta E_c(\Gamma) = a_c \varepsilon_{\text{hydro}}, \tag{1}$$

$$\Delta E_c(X) = \left(\Xi_d + \tfrac{1}{3}\Xi_u\right)\varepsilon_{\text{hydro}} - \tfrac{1}{3}\Xi_u \varepsilon_{\text{shear}}. \tag{2}$$

The material parameters used in the calculation are summarized in Table I.[12–14]

IV. RESULTS AND DISCUSSION

Figure 1(b) shows the intensity and peak energy dependences on the nanoprobe-indentation force for three typical fine PL peaks originating from individual QDs. Fine PL peaks were not observed when the nanoprobe was not indented onto the sample surface. For indentation forces from ~0.1 up to ~3.5 mN, 20–30 fine PL peaks appeared in the full PL spectrum individually, as shown in Fig. 1(a). With the indentation force increase, the intensity of the fine PL peaks increased by more than one order of magnitude and then decreased down to zero (quenched), as shown in Fig. 1(b). An almost constant blueshift was observed for each fine PL peak, ranging from 20 to 80 meV/mN. The changes in the fine PL peaks induced by indentation are reversible, i.e., the changes are retraced as the load is removed, unless the indentation does not exceed the elastic limits, as we previously reported.[7]

The blueshifts in the fine PL peaks are caused by the increase in energy band gap of InGaAs QDs evoked by the indentation-induced strain. The energy-band-gap increase is mainly due to the conduction band upward shift, which depends linearly on the hydrostatic component of the strain. The observed constant blueshift of the fine PL peaks is therefore related to the linear dependence of hydrostatic strain on the indentation force. By the calculation of strain-induced energy-band-gap increase, we can deduce the location of each QD from the rate of the blueshift of each PL peak. The details of the estimation of QD location will be reported separately, but it is approximated well (±3 nm) by (QD location in nm)=−1.59×(blueshift rate in meV/mN)

+671 nm for the QD location range from 550 to 650 nm. Most of the QDs, whose fine PL peaks were observed, were located at the 550–630 nm in QD location. This is reasonable since the PL enhancement occurs for the QDs located at around the edge of the nanoprobe (600 nm in QD location) through the strain-induced hole accumulation in the GaAs matrix (and hence in the QDs), as we discussed in our previous reports.[6,7]

The quenching of fine PL peaks cannot be attributed to the reverse mechanism of PL enhancement, i.e., hole-accumulation reduction, because the hole accumulation increases monotonically with indentation force for a nanoprobe with a flat cylindrical apex. Direct-to-indirect transition in the band lineup of the QDs and surrounding GaAs matrix is the most probable mechanism responsible for the PL quenching since the transition changes radiative QDs to nonradiative. The direct-to-indirect transition can take place for three patterns, i.e., Γ (InGaAs) versus *X* (InGaAs) crossover, Γ (QD) versus Γ (GaAs) crossover, and Γ (QD) versus *X* (GaAs) crossover. Γ (InGaAs) represents the Γ band for strained bulk InGaAs, where no quantum confinement effect is involved. On the other hand, Γ (QD) is the Γ-band quantum ground level of the InGaAs QD, which is higher than Γ (InGaAs) due to the quantum confinement effect in the QDs. When Γ (InGaAs)-X(InGaAs) crossover occurs, Γ (QD) is not the lowest energy level in the QDs anymore, but *X* (QD) becomes the ground level (reciprocally indirect). When Γ (QD) versus Γ (GaAs) crossover takes place, the electrons are not confined in the QDs anymore, but they are localized around the QDs (spatially indirect). The Γ (QD) versus *X* (GaAs) crossover brings therefore reciprocally and spatially indirect situation.

Itskevich *et al.* analyzed the intensity decrease in PL of the InAs/GaAs QDs ensemble observed in the hydrostatic pressure experiment and attributed it to the Γ (QD) versus *X* (GaAs) crossover.[15] However, unlike in the case of hydrostatic pressure experiments, the strains evoked by the nanoprobe indentation have a large shear strain component (especially at around the edge of the nanoprobe), which drastically affect the *X*-band behaviors. For the following discussion, we elucidate that the quenching of the fine PL peaks observed in our nanoprobe-indentation experiment should be attributed to the Γ (InGaAs) versus *X* (InGaAs) crossover.

The distributions of hydrostatic and shear strains and those of energy shifts in the Γ and *X* bands obtained from strain/energy-level calculations are given in Fig. 2 for the case of the QD located at the edge of the nanoprobe (600 nm in QD location) with 3.0 mN indentation. Horizontally symmetric (asymmetric) components of strain/energy-shift distributions are due to the lattice mismatch (nanoprobe indentation). It can be seen that the *X*-band shifts correspond mostly to the shear strain distribution, whereas Γ-band shifts are proportional to the hydrostatic strain. We have derived the Γ-and *X*-band levels for strained InGaAs inside the QD by volume averaging the variation in the energy shift inside the QD.[16] For the energy levels of GaAs matrix, we took also volume averaging of a 2 nm thick layer covering the QD since the energy shifts are mostly concentrated in the 2 nm thick layer, as can be seen in Fig. 2.

The band lineup diagram obtained from the above calculation is illustrated in Fig. 3 for the QD at 600 nm in QD location, with 0.0 (lattice mismatch only) and 3.0 mN indentations. Here, we assumed that the bowing parameter of the *X* band of InGaAs is 1050 meV based on a reason described later. With 3.0 mN indentation, the *X* (InGaAs) level becomes 24 meV lower than the Γ (InGaAs) level, while the *X* (GaAs) level is still higher (300–400 meV) than the Γ (QD) level. Therefore, our calculation indicates that the Γ (InGaAs) versus *X* (InGaAs) crossover takes place for the QDs with 3.0 mN indentation, whereas Γ (QD) versus *X* (GaAs) does not. The indentation force required to achieve the Γ (QD) versus *X* (GaAs) crossover was estimated to be approximately 7.4 mN [*X* (GaAs) becomes lower than Γ (GaAs) for the indentation above 6.3 mN].

In order to elucidate our Γ-*X* crossover estimation, we have compared the experimental results with the calculation as follows. From the experiments, the indentation forces required to quench the individual fine PL peaks were derived together with each QD location. On the other hand, the indentation force to evoke the Γ (InGaAs) versus *X* (InGaAs) crossover can be derived from the calculation as a function of the QD location. The experimental results and the simulation prediction are plotted together in Fig. 4. For each fine PL peak, two connected points are plotted in Fig. 4 to indicate the indentation force where the fine PL peak achieved the maximum and that where the peak disappeared. The Γ-*X* crossover should take place between the two points. The QD location is derived from the blueshift rate of each fine PL peak.

The calculation gives a curve of the boundary where the Γ (InGaAs) versus *X* (InGaAs) takes place. In order to derive the curve, we need the bowing parameter of the InGaAs *X* band. Although two values were found in references for the bowing parameter (experimentally obtained 80 meV by Kelso *et al.* [17,18] and theoretically derived 1400 meV by Porod and Ferry[19] and Adachi [20]), there seems to be no established value so far. Therefore, we treated it as a fitting parameter in our calculation. The experiments and calculation agrees well in Fig. 4 with the bowing parameter of 1050 meV. This shows that direct-to-indirect transition by the Γ (InGaAs) versus *X* (InGaAs) crossover is the mechanism of the quenching of the fine PL peaks. The best-fitted curve was obtained with the bowing parameter of the InGaAs *X* band of 1050 meV, and its deviation should be ±50 meV. The bowing parameter of 1050 ± 50 meV deduced in this study will contribute to the evaluation of the *X*-band bowing parameter of InGaAs experimentally.

Further investigations on strain nonuniformity and *L*-band behavior (as well as detailed data analysis) are required for the complete understanding of the nanoprobe-induced strain effects. The detailed reports including these issues will be presented in the near future.

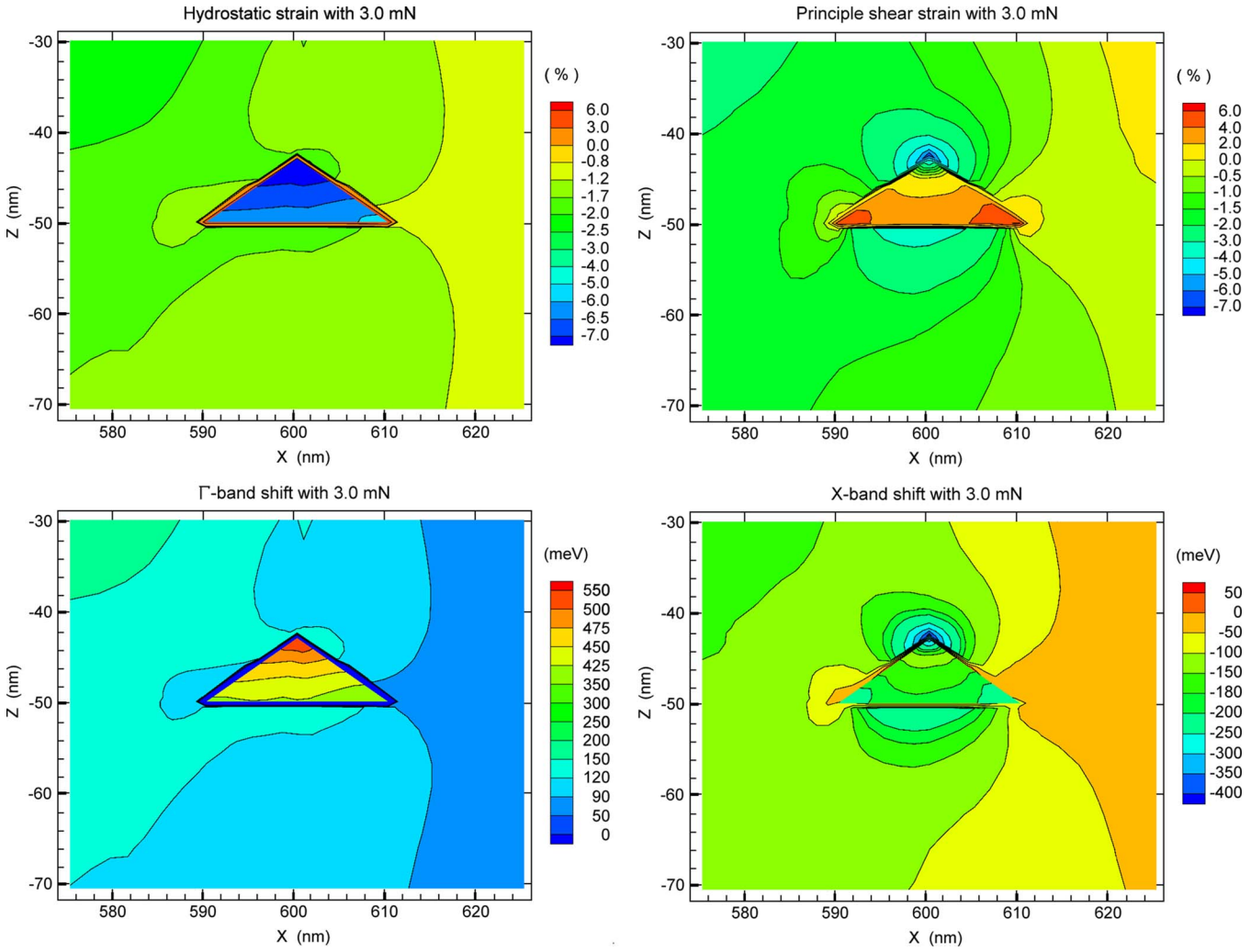

FIG. 2. (Color online) Calculated distributions of strain (hydrostatic and principle shear) and energy shift (Γ and *X* bands) for the QD located at the edge of the nanoprobe with 3.0 mN indentation.

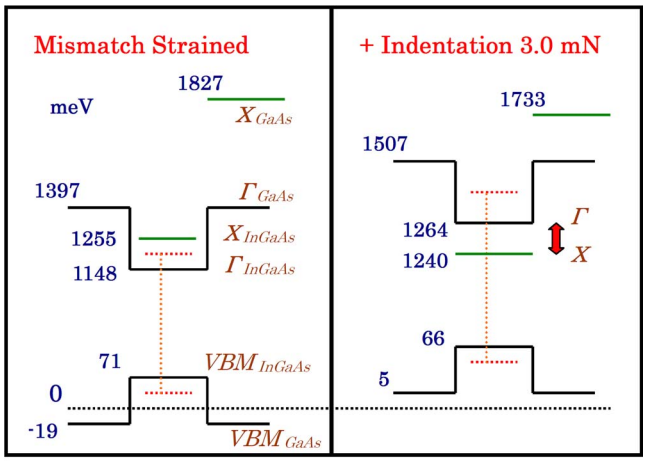

FIG. 3. (Color online) Band lineup diagram calculated for the QD located at the edge of the nanoprobe with 0.0 mN (lattice mismatched) and 3.0 mN indentations.

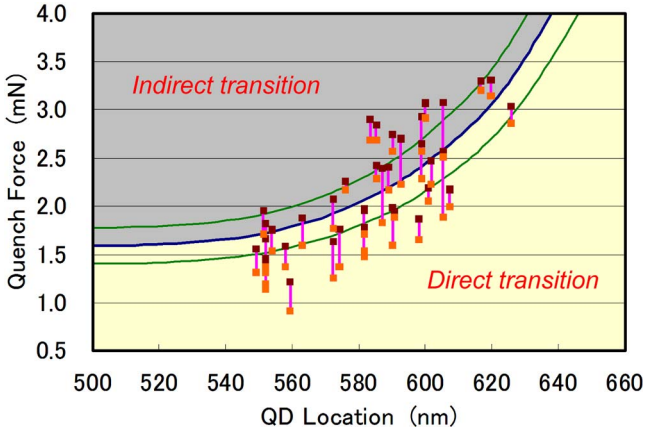

FIG. 4. (Color online) Dependence of quenching force on QD location. Experimental data are plotted as two connected points (intensity maximum and totally quenched) for each fine PL peak. The solid curves were derived from simulation with the InGaAs bowing parameters of 1000 (top), 1050 (middle), and 1100 (bottom) meV, respectively.

V. CONCLUSION

The quenching of fine PL peaks originating from individual InGaAs/GaAs QDs by nanoprobe indentation is attributed to the Γ (InGaAs) versus *X* (InGaAs) crossover. The experimentally obtained relation between the quenching indentation force and the QD location agrees well with the direct-indirect boundary predicted by the numerical simulation. The bowing parameter of 1050 ± 50 meV was deduced for the InGaAs *X* band from the experiment/simulation comparison. This result shows a high feasibility of nanoprobe-indentation experiments/simulations, in which material parameters relating to higher energy bands can be deduced with nanometer-scale resolution.

ACKNOWLEDGMENTS

The authors thank Yuta Makikawa at Saitama University of his assistance in analyzing the experimental data. The authors acknowledge financial support for this study from the Ministry of Education, Culture, Sports, Science and Technology through a Grant-in-Aid for Scientific Research (C), 20560066, 2008.

[1]A. J. Williamson, A. Franceschetti, H. Fu, L. W. Wang, and A. Zunger, J. Electron. Mater. **28**, 414 (1999).
[2]T. Dziekan, P. Zahn, V. Meded, and S. Mirbt, Phys. Rev. B **75**, 195213 (2007).
[3]J. Ahopelto, A. Yamaguchi, K. Nishi, A. Usui, and H. Sakaki, Jpn. J. Appl. Phys., Part 2 **32**, L32 (1993).
[4]D. Leonard, M. Krishnamurthy, S. Fafard, J. L. Merz, and P. M. Petroff, J. Vac. Sci. Technol. B **12**, 1063 (1994).
[5]K. Ozasa, Y. Aoyagi, A. Yamane, and Y. Arai, Appl. Phys. Lett. **83**, 2247 (2003).
[6]Y. H. Liang, M. Ohashi, Y. Arai, and K. Ozasa, Phys. Rev. B **75**, 195318 (2007).
[7]K. Ozasa, M. Maeda, M. Hara, M. Ohashi, Y. H. Liang, H. Kakoi, and Y. Arai, Physica E (Amsterdam) **40**, 1920 (2008).
[8]K. Ozasa and Y. Aoyagi, J. Cryst. Growth **188**, 370 (1998).
[9]K. Ozasa, Y. Aoyagi, M. Iwaki, and H. Kurata, J. Appl. Phys. **94**, 313 (2003).
[10]K. Ozasa, S. Nomura, and Y. Aoyagi, Superlattices Microstruct. **30**, 169 (2001).
[11]G. E. Pikus and G. L. Bir, Sov. Phys. Solid State **1**, 1502 (1959).
[12]C. G. Van de Walle, Phys. Rev. B **39**, 1871 (1989).
[13]M. C. Munoz and G. Armelles, Phys. Rev. B **48**, 2839 (1993).
[14]I. Vurgaftman, J.R. Meyer, and L. R. Ram-Mohan, J. Appl. Phys. **89**, 5815 (2001).
[15]I. E. Itskevich, S. G. Lyapin, I. A. Troyan, P. C. Klipstein, L. Eaves, P. C. Main, and M. Henini, Phys. Rev. B **58**, R4250 (1998).
[16]C. E. Pryor and M.-E. Pistol, Phys. Rev. B **72**, 205311 (2005).
[17]S. M. Kelso, D. E. Aspnes, C. G. Olson, D. W. Lynch, and K. J. Bachmann, Proc. SPIE **452**, 100 (1984).
[18]*Numerical Data and Functional Relationship in Science and Technology*, Landölt-Bornstein, New Series, Group III, Vol. 22 (Springer, Berlin, 1987).
[19]W. Porod and D. K. Ferry, Phys. Rev. B **27**, 2587 (1983).
[20]S. Adachi, J. Appl. Phys. **61**, 4869 (1987).